

# Electronic structure and magnetic properties of pyridinophane complexes of iron with radical-bearing catecholates: a quantum chemical study\*

V. I. Minkin, A. A. Starikova,<sup>\*</sup> M. G. Chegrev, and A. G. Starikov

Institute of Physical and Organic Chemistry at Southern Federal University,  
194/2 prosp. Stachki, 344090 Rostov-on-Don, Russian Federation.  
E-mail: aastarikova@sfedu.ru

A computer simulation of the structure, energy characteristics, and magnetic properties of mononuclear iron(III) complexes with *N,N'*-substituted 2,11-diaza[3.3]-(2,6)pyridinophane bases and *o*-benzoquinone ligands containing nitroxyl and TEMPO radicals was carried out at the UTPSSh/6-311++G(d,p) level of the density functional theory. The dependence of the character of exchange interactions between paramagnetic centers on the nature of the radical group was revealed. It was found that the energy differences between the isomers of compounds studied are determined by the bulkiness of the alkyl substituent at nitrogen atoms of the tetraazamacrocyclic ligands. Systems potentially capable of manifesting thermally initiated spin crossover were found.

**Key words:** iron complexes, catecholates, stable radicals, spin crossover, magnetic properties, quantum chemical modeling, density functional theory.

The design of advanced materials for molecular electronics and spintronics devices is a topical avenue of modern chemical research.<sup>1–3</sup> Open-shell complexes whose properties vary depending on external factors are used as building blocks for molecular switches and spin qubits.<sup>4–10</sup> Currently, there is considerable research activity aimed at searching for promising magnetically active molecules.<sup>1–21</sup>

Spin crossover (SCO) is the most widespread magnetic bistability mechanism of transition-metal complexes.<sup>22</sup> The effect is realized through (intra)electronic transitions between the low-spin (LS) and high-spin (HS) states of the central ion induced by temperature, pressure, magnetic field or irradiation. Most often, SCO occurs in iron(II) complexes.<sup>23</sup> There are also iron(III)<sup>24</sup> and other metal compounds<sup>25,26</sup> that demonstrate SCO behavior. The advantage of the trivalent iron complexes over Fe<sup>II</sup>-based systems consists in that all spin states are paramagnetic. In these compounds, the ligand field strength appropriate for SCO to occur is achieved by properly engineering the Fe<sup>III</sup>N<sub>4</sub>O<sub>2</sub> coordination site.

A series of studies<sup>27–32</sup> on the ability of salt-like *o*-benzoquinone complexes of iron with tris(2-pyridylmethyl)amine derivatives to demonstrate changes in the magnetic properties upon SCO was followed by a research into an iron(III) complex with tris(2-pyridylmethyl)amine base and a catecholate (Cat) bearing a nitronyl nitroxide substituent.<sup>33</sup> The presence of a stable radical group in the

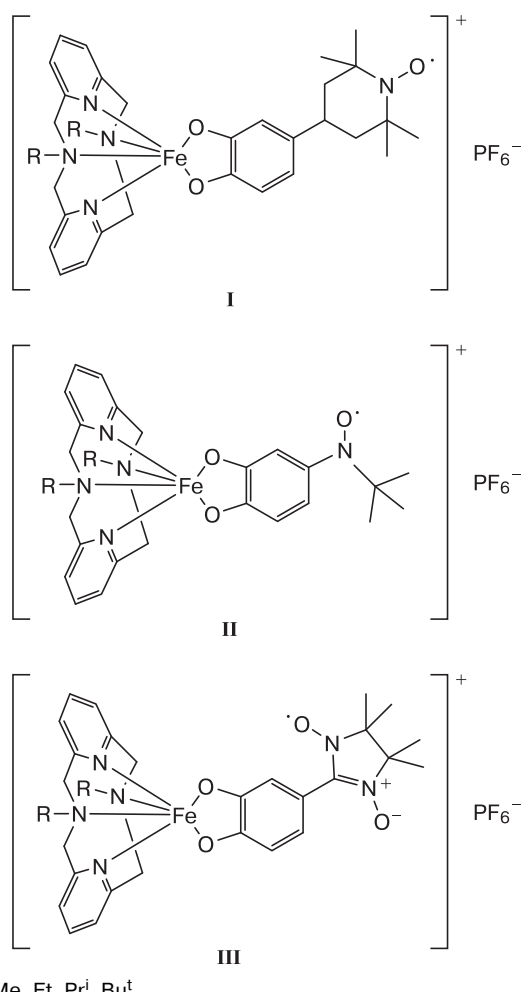
compound in question<sup>33</sup> and in other transition-metal compounds<sup>34–41</sup> causes the occurrence of additional exchange interactions, which allows one to expect extension of the application field of such systems.

Recently,<sup>42,43</sup> we predicted the possibility for SCO to occur in the experimentally characterized *o*-benzoquinone complexes of iron with *N,N'*-dimethyl-2,11-diaza[3.3]-(2,6)pyridinophane derivatives.<sup>44,45</sup> By varying the alkyl substituents in the tetraazamacrocyclic ligand of such compounds one can vary the energy difference between the LS and HS electronic isomers (electromers<sup>53</sup>), which specifies the aptitude of a molecule to undergo thermally initiated SCO.<sup>46–52</sup> In this work, in order to search for novel magnetically active systems, we carried out a computer simulation of the geometry and electronic structure, as well as the energy characteristics and magnetic properties of type-I–III iron complexes (R = Me, Et, Pr<sup>i</sup>, Bu<sup>t</sup>) with *N,N'*-dialkyl-substituted pyridinophane bases and *o*-benzoquinones bearing various radical groups including TEMPO, *tert*-butyl nitroxide (TBN), and 4,4,5,5-tetramethyl-4,5-dihydro-1*H*-imidazol-1-oxyl-3-oxide (nitronyl nitroxide, NN).

## Calculation Procedure

Calculations were carried out in terms of the density functional theory (DFT) using the Gaussian 16 program,<sup>54</sup> the UTPSSh functional,<sup>55,56</sup> and the 6-311++G(d,p) extended basis set. This combination is known to provide a correct reproduction of the energy and magnetic characteristics of the com-

\* Dedicated to Academician of the Russian Academy of Sciences V. N. Charushin on the occasion of his 70th birthday.



$R = \text{Me, Et, Pr}^i, \text{Bu}^t$

plexes with redox-active ligands demonstrating magnetic bistability.<sup>47–49,51,57</sup> According to calculations of the experimentally studied iron compounds, SCO is expected to occur at  $\Delta E_{\text{HS}-\text{LS}} < 10 \text{ kcal mol}^{-1}$ . Since DFT studies of transition-metal complexes with redox-active ligands require taking account of outer-sphere counterions,<sup>58</sup> in this work we performed quantum chemical calculations of compounds containing a hexafluorophosphate anion whose orientation and position were specified using the X-ray data for structurally similar compounds.<sup>51</sup> Stationary points on the potential energy surfaces (PES) were located by full geometry optimization of the molecular structures without symmetry constraints. Calculations involved stability tests of the DFT wavefunctions and determination of force constants. Since the calculated atomic charges provide no reliable information on the oxidation state of the central ion in the complexes with redox-active ligands, this parameter was estimated from the spin density distribution.<sup>58</sup> The exchange constants were calculated within the "broken symmetry" (BS) formalism<sup>59</sup> using the Yamaguchi formula.<sup>60</sup> The molecular structures were visualized using the ChemCraft program.<sup>61</sup>

## Results and Discussion

Geometry optimization of type-I complex ( $R = \text{Me}$ ) led to structure **1** (Fig. 1, Table 1) corresponding to

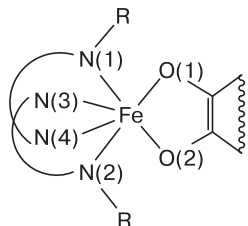


**Fig. 1.** Atomic numbering scheme for the coordination site of type-I–III complexes ( $R = \text{Me, Et, Pr}^i, \text{Bu}^t$ ).

a minimum on the triplet PES. The bond lengths in the redox-active fragment of structure **1** are close to those in the LS isomer of a structurally similar compound containing no radical substituent in the *o*-benzoquinone ring,<sup>42</sup> being intermediate between the characteristic distances for the semiquinonate and Cat forms of the ligand in the transition-metal complexes with *o*-quinone derivatives.<sup>46,49,62–64</sup> An analysis of the spin density distribution (Fig. 2) and coordination site geometry (see Table 1) suggests that the electronic structure of isomer **1** can be described as  ${}_{\text{LS}}\text{Fe}^{\text{III}}\text{Cat-TEMPO}$ . The HS electromer **2** of the complex in question bears a paramagnetic center on the TEMPO substituent and five unpaired electrons on the iron ion. The electron density is partially displaced from the metal to the adjacent donor O atoms (see Fig. 2). This is similar to the situation<sup>49</sup> where the conclusion that the structure contains a trivalent metal ion and the Cat form of the ligand was substantiated by Mössbauer spectroscopy, X-ray diffraction, and magnetic measurements data. This circumstance, as well as the Fe–N(3) and Fe–N(4) bond lengths that are shorter than the corresponding distances in the iron(II) complexes<sup>23</sup> (see Table 1), suggest that electromer **2** contains an  ${}_{\text{HS}}\text{Fe}^{\text{III}}$  ion and the Cat moiety.

Variation of alkyl groups at nitrogen atoms of the tetraazamacrocyclic base does not lead to changes in the electronic structure of the complexes, *viz.*, the electromers of the type-I complexes ( $R = \text{Et, Pr}^i, \text{Bu}^t$ ) also contain the dianionic form of *o*-benzoquinone and  $\text{Fe}^{\text{III}}$  ions in both LS and HS states (isomers **3, 5, 7** and isomers **4, 6, 8**, respectively). From the data of Table 1 it follows that an increase in the size of the substituent R has little effect on the Fe–O(1), Fe–O(2), Fe–N(3), and Fe–N(4) distances, namely, the bond lengths vary within 0.010 Å except isomer **7** ( ${}_{\text{LS}}\text{Fe}^{\text{III}}\text{Cat-TEMPO}$ ) of type-I compound ( $R = \text{Bu}^t$ ) where the Fe–N(3) and Fe–N(4) contacts are 0.020 Å longer than those in electromer **1** ( ${}_{\text{LS}}\text{Fe}^{\text{III}}\text{Cat-TEMPO}$ ). Noteworthy is a large (by more than 0.100 Å) elongation of the Fe–N(1) and Fe–N(2) bonds on going from the complex with methyl-substituted tetraazamacrocyclic base to the compound with *tert*-butyl derivative of pyridinophane. Steric hindrances produced by bulky alkyl substituents at nitrogen atoms of the tetradentate base make the formation of shorter coordination bonds

**Table 1.** Coordination bond lengths (in Å) in electromers of type-I–III complexes ( $R = \text{Me, Et, Pr}^i, \text{Bu}^t$ ) obtained from UTPSSh/6-311++G(d,p) calculations

Complex	R	Electromer	Fe—O(1)	Fe—O(2)	Fe—N(1)	Fe—N(2)	Fe—N(3)	Fe—N(4)
<b>I</b>	Me	<b>1</b> ( ${}_{\text{LS}}\text{Fe}^{\text{III}}\text{Cat—TEMPO}$ )	1.893	1.892	2.039	2.040	1.901	1.901
		<b>2</b> ( ${}_{\text{HS}}\text{Fe}^{\text{III}}\text{Cat—TEMPO}$ )	1.950	1.949	2.262	2.257	2.091	2.093
	Et	<b>3</b> ( ${}_{\text{LS}}\text{Fe}^{\text{III}}\text{Cat—TEMPO}$ )	1.895	1.891	2.051	2.051	1.900	1.900
		<b>4</b> ( ${}_{\text{HS}}\text{Fe}^{\text{III}}\text{Cat—TEMPO}$ )	1.951	1.947	2.265	2.270	2.086	2.089
	$\text{Pr}^i$	<b>5</b> ( ${}_{\text{LS}}\text{Fe}^{\text{III}}\text{Cat—TEMPO}$ )	1.898	1.892	2.076	2.077	1.906	1.905
		<b>6</b> ( ${}_{\text{HS}}\text{Fe}^{\text{III}}\text{Cat—TEMPO}$ )	1.957	1.952	2.290	2.295	2.088	2.087
	$\text{Bu}^t$	<b>7</b> ( ${}_{\text{LS}}\text{Fe}^{\text{III}}\text{Cat—TEMPO}$ )	1.892	1.889	2.174	2.173	1.921	1.920
		<b>8</b> ( ${}_{\text{HS}}\text{Fe}^{\text{III}}\text{Cat—TEMPO}$ )	1.959	1.955	2.363	2.371	2.092	2.094
<b>II</b>	Me	<b>9</b> ( ${}_{\text{LS}}\text{Fe}^{\text{III}}\text{Cat—TBN}$ )	1.888	1.896	2.039	2.038	1.901	1.903
		<b>10</b> ( ${}_{\text{HS}}\text{Fe}^{\text{III}}\text{Cat—TBN}$ )	1.948	1.952	2.255	2.258	2.094	2.089
	Et	<b>11</b> ( ${}_{\text{LS}}\text{Fe}^{\text{III}}\text{Cat—TBN}$ )	1.888	1.897	2.051	2.051	1.899	1.901
		<b>12</b> ( ${}_{\text{HS}}\text{Fe}^{\text{III}}\text{Cat—TBN}$ )	1.948	1.952	2.269	2.263	2.090	2.084
	$\text{Pr}^i$	<b>13</b> ( ${}_{\text{LS}}\text{Fe}^{\text{III}}\text{Cat—TBN}$ )	1.892	1.897	2.076	2.075	1.905	1.906
		<b>14</b> ( ${}_{\text{HS}}\text{Fe}^{\text{III}}\text{Cat—TBN}$ )	1.954	1.959	2.289	2.290	2.089	2.084
	$\text{Bu}^t$	<b>15</b> ( ${}_{\text{LS}}\text{Fe}^{\text{III}}\text{Cat—TBN}$ )	1.885	1.895	2.179	2.172	1.921	1.923
		<b>16</b> ( ${}_{\text{HS}}\text{Fe}^{\text{III}}\text{Cat—TBN}$ )	1.957	1.958	2.370	2.362	2.094	2.090
<b>III</b>	Me	<b>17</b> ( ${}_{\text{LS}}\text{Fe}^{\text{III}}\text{Cat—NN}$ )	1.886	1.898	2.038	2.038	1.900	1.903
		<b>18</b> ( ${}_{\text{HS}}\text{Fe}^{\text{III}}\text{Cat—NN}$ )	1.942	1.961	2.255	2.265	2.089	2.093
	Et	<b>19</b> ( ${}_{\text{LS}}\text{Fe}^{\text{III}}\text{Cat—NN}$ )	1.885	1.900	2.051	2.051	1.899	1.901
		<b>20</b> ( ${}_{\text{HS}}\text{Fe}^{\text{III}}\text{Cat—NN}$ )	1.941	1.961	2.266	2.264	2.085	2.088
	$\text{Pr}^i$	<b>21</b> ( ${}_{\text{LS}}\text{Fe}^{\text{III}}\text{Cat—NN}$ )	1.888	1.901	2.075	2.077	1.904	1.905
		<b>22</b> ( ${}_{\text{HS}}\text{Fe}^{\text{III}}\text{Cat—NN}$ )	1.947	1.967	2.289	2.294	2.085	2.087
	$\text{Bu}^t$	<b>23</b> ( ${}_{\text{LS}}\text{Fe}^{\text{III}}\text{Cat—NN}$ )	1.884	1.899	2.172	2.175	1.919	1.921
		<b>24</b> ( ${}_{\text{HS}}\text{Fe}^{\text{III}}\text{Cat—NN}$ )	1.951	1.950	2.362	2.371	2.091	2.091

*Note.* For atomic numbering scheme, see Fig. 1.

impossible. These changes in the geometry of the coordination site destabilize the LS electromers of the complexes and, as a consequence, are reflected in the relative energies of the isomers. As the bulkiness of the alkyl substituent in

the tetraazamacrocyclic increases, the energy difference between the ground states  ${}_{\text{LS}}\text{Fe}^{\text{III}}\text{Cat—TEMPO}$  and the HS isomers  ${}_{\text{HS}}\text{Fe}^{\text{III}}\text{Cat—TEMPO}$  of type-I systems ( $R = \text{Me, Et, Pr}^i, \text{Bu}^t$ ) decreases from 10.3 to 1.7 kcal mol<sup>-1</sup> taking

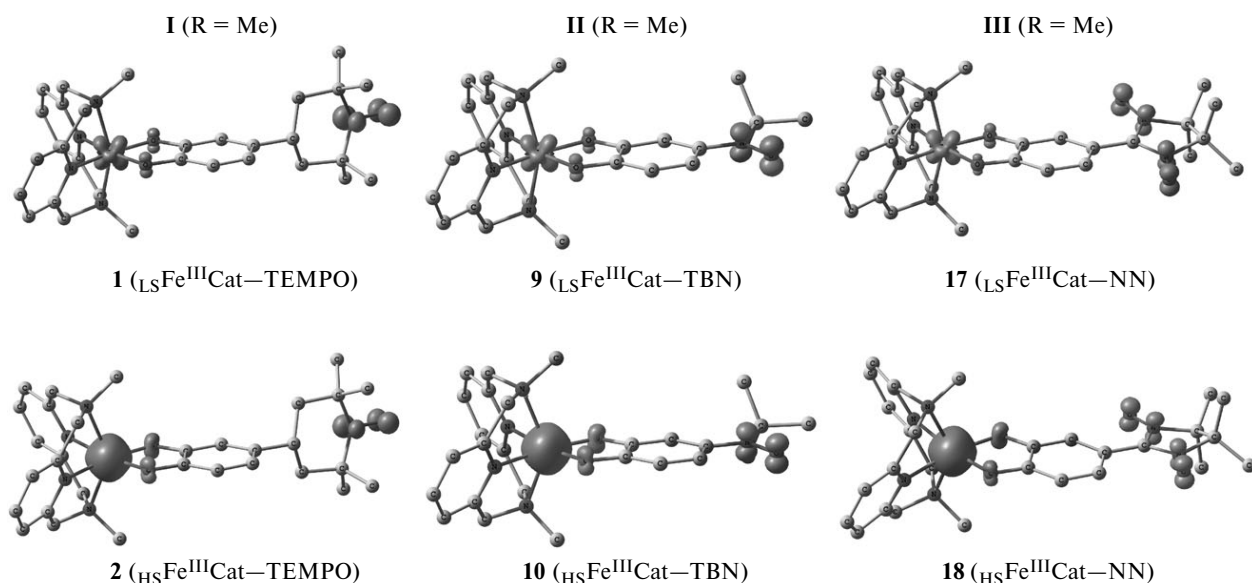


**Fig. 2.** Spin density distributions in electromers of type-I–III complexes ( $R = \text{Me}$ ) obtained from UTPSSh/6-311++G(d,p) calculations. Here and in Fig. 3 hydrogen atoms and  $\text{PF}_6^-$  anion are omitted; the contour value is 0.03 e Å<sup>-3</sup>.

**Table 2.** Spins ( $S$ ), relative energies calculated without ( $\Delta E$ ) and with inclusion of zero-point vibrational energy correction ( $\Delta E^{ZPE}$ ), and exchange coupling parameters ( $J$ ) in electromers of type-I–III complexes ( $R = \text{Me, Et, Pr}^i, \text{Bu}^t$ ) obtained from density functional UTPSSh/6-311++G(d,p) calculations

Complex	R	Electromer	$S$	$\Delta E$	$\Delta E^{ZPE}$	$J$ kcal mol $^{-1}$ /cm $^{-1}$
				kcal mol $^{-1}$	/cm $^{-1}$	
I	Me	1 ( ${}_{\text{LS}}\text{Fe}^{\text{III}}\text{Cat}$ —TEMPO)	1	0.0	0.0	0
		2 ( ${}_{\text{HS}}\text{Fe}^{\text{III}}\text{Cat}$ —TEMPO)	3	12.2	10.3	0
	Et	3 ( ${}_{\text{LS}}\text{Fe}^{\text{III}}\text{Cat}$ —TEMPO)	1	0.0	0.0	0
		4 ( ${}_{\text{HS}}\text{Fe}^{\text{III}}\text{Cat}$ —TEMPO)	3	11.8	10.1	0
	Pr $^i$	5 ( ${}_{\text{LS}}\text{Fe}^{\text{III}}\text{Cat}$ —TEMPO)	1	0.0	0.0	0
		6 ( ${}_{\text{HS}}\text{Fe}^{\text{III}}\text{Cat}$ —TEMPO)	3	9.0	7.1	0
	Bu $^t$	7 ( ${}_{\text{LS}}\text{Fe}^{\text{III}}\text{Cat}$ —TEMPO)	1	0.0	0.0	0
		8 ( ${}_{\text{HS}}\text{Fe}^{\text{III}}\text{Cat}$ —TEMPO)	3	3.7	1.7	0
II	Me	9 ( ${}_{\text{LS}}\text{Fe}^{\text{III}}\text{Cat}$ —TBN)	1	0.0	0.0	-826
		10 ( ${}_{\text{HS}}\text{Fe}^{\text{III}}\text{Cat}$ —TBN)	3	12.4	10.5	-376
	Et	11 ( ${}_{\text{LS}}\text{Fe}^{\text{III}}\text{Cat}$ —TBN)	1	0.0	0.0	-768
		12 ( ${}_{\text{HS}}\text{Fe}^{\text{III}}\text{Cat}$ —TBN)	3	12.1	10.0	-355
	Pr $^i$	13 ( ${}_{\text{LS}}\text{Fe}^{\text{III}}\text{Cat}$ —TBN)	1	0.0	0.0	-773
		14 ( ${}_{\text{HS}}\text{Fe}^{\text{III}}\text{Cat}$ —TBN)	3	9.3	7.1	-363
	Bu $^t$	15 ( ${}_{\text{LS}}\text{Fe}^{\text{III}}\text{Cat}$ —TBN)	1	0.0	0.0	-758
		16 ( ${}_{\text{HS}}\text{Fe}^{\text{III}}\text{Cat}$ —TBN)	3	3.7	2.1	-363
III	Me	17 ( ${}_{\text{LS}}\text{Fe}^{\text{III}}\text{Cat}$ —NN)	1	0.0	0.0	180
		18 ( ${}_{\text{HS}}\text{Fe}^{\text{III}}\text{Cat}$ —NN)	3	12.4	10.5	46
	Et	19 ( ${}_{\text{LS}}\text{Fe}^{\text{III}}\text{Cat}$ —NN)	1	0.0	0.0	161
		20 ( ${}_{\text{HS}}\text{Fe}^{\text{III}}\text{Cat}$ —NN)	3	12.0	10.1	47
	Pr $^i$	21 ( ${}_{\text{LS}}\text{Fe}^{\text{III}}\text{Cat}$ —NN)	1	0.0	0.0	161
		22 ( ${}_{\text{HS}}\text{Fe}^{\text{III}}\text{Cat}$ —NN)	3	9.4	7.6	43
	Bu $^t$	23 ( ${}_{\text{LS}}\text{Fe}^{\text{III}}\text{Cat}$ —NN)	1	0.0	0.0	168
		24 ( ${}_{\text{HS}}\text{Fe}^{\text{III}}\text{Cat}$ —NN)	3	4.0	2.0	40

account the zero-point vibrational energy (ZPE) correction (Table 2). The results obtained allow one to expect the occurrence of thermally induced SCO at iron ions.

The **1** ( ${}_{\text{LS}}\text{Fe}^{\text{III}}\text{Cat}$ —TEMPO)  $\rightleftharpoons$  **2** ( ${}_{\text{HS}}\text{Fe}^{\text{III}}\text{Cat}$ —TEMPO) transition of the complex with the methyl-substituted pyridinophane derivative can occur only partially due to significant destabilization of the HS electrome. As to the type-I compound with  $R = \text{Bu}^t$ , the packing effects ignored in single-molecule DFT calculations can lead to a situation where the complex will be in the  ${}_{\text{HS}}\text{Fe}^{\text{III}}\text{Cat}$ —TEMPO state (structure **8** on the septet PES) in a wide temperature range. A comparison of the energy difference calculated for the type-I compound with  $R = \text{Me}$  with that reported for the related complex with unsubstituted *o*-benzoquinone ( $\Delta E = 11.4$  kcal mol $^{-1}$  without inclusion of ZPE correction)<sup>42</sup> shows that the radical group has little effect on the energy characteristics of such systems.

The results of calculations of the BS states and subsequent evaluation of the exchange constants  $J$  for type-I complexes ( $R = \text{Me, Et, Pr}^i, \text{Bu}^t$ ) suggest that there is no exchange between the spins of the unpaired electrons of the iron ion and the paramagnetic substituent (see Table 2). This is in excellent agreement with the results of a study<sup>65</sup> of exchange in compounds containing the TEMPO radical. The spin density of the radical group is localized at the nitrogen and oxygen atoms and separated from the quinone ring  $\pi$ -system by aliphatic bridges (see Fig. 2), which precludes the formation of an exchange channel (Fig. 3). Therefore, the SCO transitions of the type-I complexes with  $R = \text{Me, Et, Pr}^i$ , and  $\text{Bu}^t$  will be accompanied by changes in the total spin of the system from  $S = 1$  to  $S = 3$ . This type of molecules can find applications in the molecular design of spin qubits or some other devices utilizing two noninteracting paramagnetic centers.

From the results of calculations (see Fig. 2, Tables 1 and 2) it follows that electromers of the type-II and type-III complexes ( $R = \text{Me, Et, Pr}^i$ , and  $\text{Bu}^t$  for both types) contain  $\text{Fe}^{\text{III}}$  ions and the Cat form of the redox ligand,

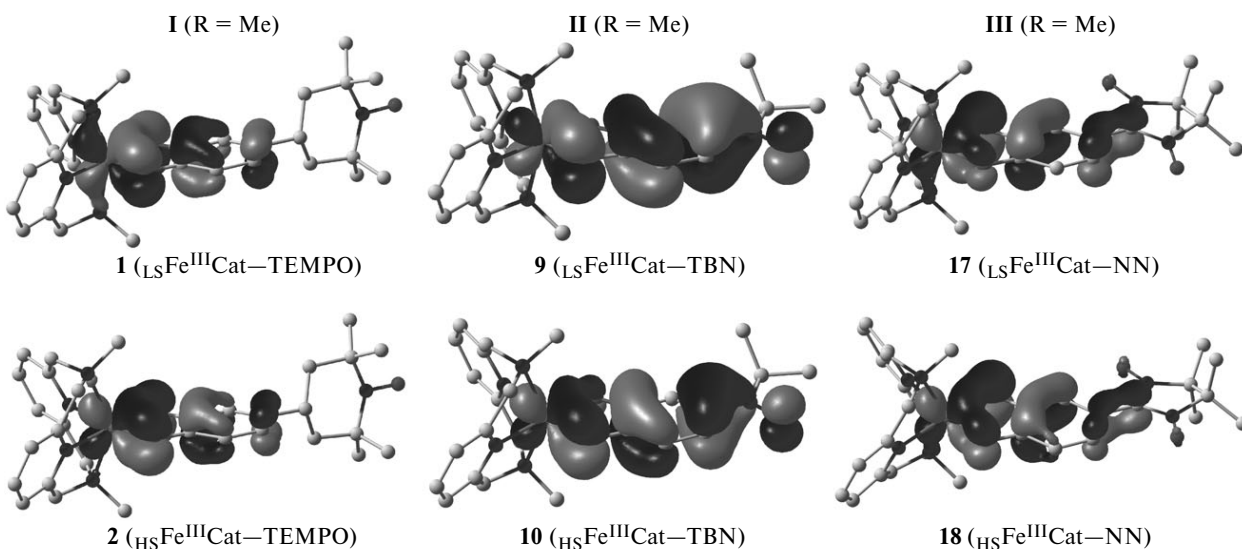


**Fig. 3.** Visualization of magnetic orbitals in electromers of type-I–III complexes ( $R = \text{Me}$ ) obtained from UTPSSh/6-311++G(d,p) calculations.

just like the type-**I** compounds ( $R = \text{Me, Et, Pr}^i, \text{Bu}^t$ ). An analysis of the results obtained suggests that the geometric parameters of the coordination site and, as a consequence, the relative energies of the isomers of the complexes in question are almost independent of the type of the radical substituent in the catecholate moiety, *viz.*, the type-**II** and type-**III** compounds with nitroxyl substituents can potentially feature a SCO behavior. The type of the radical specifies the strength and character of exchange interactions. For instance, although the unpaired electrons of the metal and the TBN substituent in the electromers of the type-**II** complexes ( $R = \text{Me, Et, Pr}^i, \text{Bu}^t$ ) with the *o*-benzoquinone containing *tert*-butyl nitroxide are separated by sufficiently long distances (see Fig. 2), the contributions of the iron atom, quinone ring, and TBN to the magnetic orbital provide the formation of an exchange channel and, therefore, the occurrence of antiferromagnetic interactions (see Fig. 3). The predicted strong anti-ferromagnetic coupling (see Table 2) leads to diamagnetism of the LS states **9, 11, 13, 15** by analogy with the iron bischelate adducts with diiminobenzoquinones studied earlier.<sup>66</sup> In the type-**III** compounds ( $R = \text{Me, Et, Pr}^i, \text{Bu}^t$ ) the orbitals of the iron atom and nitronyl nitroxide do not overlap, namely, the nitrogen and oxygen atoms of the NN radical do not contribute to the magnetic orbital (see Fig. 3), which predictably<sup>67</sup> leads to ferromagnetic coupling. The LS isomers **17, 19, 21**, and **23** are characterized by strong exchange, while the HS electromers **18, 20, 22**, and **24** are characterized by moderate ferromagnetic interactions. Therefore, electromers of the type-**III** complexes ( $R = \text{Me, Et, Pr}^i, \text{Bu}^t$ ) are expected to exhibit the properties of paramagnetics and the SCO transitions between them will be accompanied by significant changes in the magnetic properties. Such systems can find application as building blocks for molecular electronics and spintronics devices.

Summing up, our DFT study of mononuclear iron complexes with *N,N'*-dialkyl-2,11-diaza[3.3]-(2,6)pyridinophanes and *o*-benzoquinone ligands bearing TEMPO, *tert*-butyl nitroxide, and nitronyl nitroxide radicals revealed that the energy difference between electromers of the compounds under examination depends on the size of the alkyl substituent in the tetraazamacrocycle, being independent of the presence and type of the radical group. The predicted energy characteristics allow one to expect the occurrence of thermally initiated SCO at  $\text{Fe}^{III}$  ions in the systems under examination, which will be accompanied by changes in the magnetic properties. Based on the results of calculations, other expectations are as follows: no exchange between paramagnetic centers in the complexes with the TEMPO radical, strong antiferromagnetic exchange interactions in the complexes with *tert*-butyl nitroxide, and ferromagnetic coupling between the spins of the unpaired electrons in the systems with the nitronyl nitroxide substituent. The use of synthetically available structural motifs in the calculations of the type-**I–III** complexes as

well as the diverse chemistry of stable radicals<sup>68–70</sup> offer great prospects for the synthesis of novel compounds thus engineered.

This work was financially supported by the Russian Science Foundation (Project No. 19-73-00090).

This paper does not contain descriptions of studies on animals or humans.

The authors declare no competing interests.

## References

- O. Sato, *Nat. Chem.*, 2016, **8**, 644.
- K. Senthil Kumar, M. Ruben, *Coord. Chem. Rev.*, 2017, **346**, 176.
- E. Coronado, *Nat. Rev. Mater.*, 2020, **5**, 87.
- A. Dei, D. Gatteschi, C. Sangregorio, L. Sorace, *Acc. Chem. Res.*, 2004, **37**, 827.
- O. Sato, J. Tao, Yu.-Z. Zhang, *Angew. Chem., Int. Ed.*, 2007, **46**, 2152.
- V. I. Minkin, *Russ. Chem. Bull.*, 2008, **57**, 687.
- G. A. Timco, T. B. Faust, F. Tuna, R. E. P. Winpenny, *Chem. Soc. Rev.*, 2011, **40**, 3067.
- G. Aromi, P. Gamez, O. Roubeau, in *Spin States in Biochemistry and Inorganic Chemistry: Influence on Structure and Reactivity*, Eds M. Swart, M. Costas, John Wiley & Sons, 2016, p. 263.
- M. M. Khusniyarov, *Chem. — Eur. J.*, 2016, **22**, 15178.
- O. Drath, C. Boskovic, *Coord. Chem. Rev.*, 2018, **375**, 256.
- A. I. Poddel'sky, V. K. Cherkasov, G. A. Abakumov, *Coord. Chem. Rev.*, 2009, **293**, 291.
- M. V. Fedin, S. L. Veber, E. G. Bagryanskaya, V. I. Ovcharenko, *Coord. Chem. Rev.*, 2015, **289–290**, 341.
- A. A. Starikova, V. I. Minkin, *Russ. Chem. Rev.*, 2018, **87**, 1049.
- A. V. Piskunov, K. I. Pashanova, I. V. Ershova, A. S. Bogomyakov, A. G. Starikov, G. K. Fukin, *Russ. Chem. Bull.*, 2019, **68**, 757.
- N. A. Protasenko, A. I. Poddel'sky, A. S. Bogomyakov, A. G. Starikov, I. V. Smolyaninov, N. T. Berberova, G. K. Fukin, V. K. Cherkasov, *Inorg. Chim. Acta*, 2019, **489**, 1.
- Yu. A. Ten, N. M. Troshkova, E. V. Tretyakov, *Russ. Chem. Rev.*, 2020, **89**, 693.
- D. S. Yambulatov, S. A. Nikolaevskii, M. A. Kiskin, T. V. Magdesieva, O. A. Levitskiy, D. V. Korchagin, N. N. Efimov, P. N. Vasil'ev, A. S. Goloveshkin, A. A. Sidorov, I. L. Eremenko, *Molecules*, 2020, **25**, 2054.
- I. Nikovskiy, A. Polezhaev, V. Novikov, D. Aleshin, A. Pavlov, E. Saffiulina, R. Aysin, P. Dorovatovskii, L. Nodaraki, F. Tuna, Yu. Nelyubina, *Chem. — Eur. J.*, 2020, **26**, 5629.
- I. V. Ershova, A. V. Piskunov, V. K. Cherkasov, *Russ. Chem. Rev.*, 2020, **89**, 1157.
- A. Palii, S. Aldoshin, B. Tsukerblat, *Coord. Chem. Rev.*, 2021, **426**, 213555.
- V. I. Ovcharenko, O. V. Kuznetsova, *Russ. Chem. Rev.*, 2020, **89**, 1261.
- Spin-Crossover Materials: Properties and Applications*, Ed. M. A. Halcrow, John Wiley & Sons, Chichester, 2013, 564 pp.
- M. A. Halcrow, *Polyhedron*, 2007, **26**, 3523.
- D. J. Harding, P. Harding, W. Phonsri, *Coord. Chem. Rev.*, 2016, **313**, 38.

25. I. Krivokapic, M. Zerara, M. L. Daku, A. Vargas, C. Enachescu, C. Ambrus, P. Tregenna-Piggott, N. Amstutz, E. Krausz, A. Hauser, *Coord. Chem. Rev.*, 2007, **251**, 364.
26. A. V. Vologzhanina, A. S. Belov, V. V. Novikov, A. V. Dolganov, G. V. Romanenko, V. I. Ovcharenko, A. A. Korlyukov, M. I. Buzin, Ya. Z. Voloshin, *Inorg. Chem.*, 2015, **54**, 5827.
27. A. J. Simaan, M.-L. Boillot, R. Carrasco, J. Cano, J.-J. Girerd, T. A. Mattioli, J. Ensling, H. Spiering, P. Gutlich, *Chem. — Eur. J.*, 2005, **11**, 1779.
28. S. Floquet, A. J. Simaan, E. Rivière, M. Nierlich, P. Thuéry, J. Ensling, P. Gutlich, J.-J. Girerd, M.-L. Boillot, *Dalton Trans.*, 2005, 1734.
29. C. Enachescu, A. Hauser, J.-J. Girerd, M.-L. Boillot, *ChemPhysChem*, 2006, **7**, 1127.
30. J.-J. Girerd, M.-L. Boillot, G. Blain, E. Rivière, *Inorg. Chim. Acta*, 2008, **361**, 4012.
31. W. Kaszub, M. Buron-Le Cointe, M. Lorenc, M.-L. Boillot, M. Servol, A. Tissot, L. Guérin, H. Cailleau, E. Collet, *Eur. J. Inorg. Chem.*, 2013, 992.
32. A. Tissot, H. J. Shepherd, L. Toupet, E. Collet, J. Sainton, G. Molnár, P. Guionneau, M.-L. Boillot, *Eur. J. Inorg. Chem.*, 2013, 1001.
33. C. R. Tichnell, D. A. Shultz, C. V. Popescu, I. Sokirniy, P. D. Boyle, *Inorg. Chem.*, 2015, **54**, 4466.
34. M. L. Kirk, D. A. Shultz, *Coord. Chem. Rev.*, 2013, **257**, 218.
35. N. A. Artiukhova, K. Yu. Maryunina, S. V. Fokin, E. V. Tretyakov, G. V. Romanenko, A. V. Polushkin, A. S. Bogomyakov, R. Z. Sagdeev, V. I. Ovcharenko, *Russ. Chem. Bull.*, 2013, **62**, 2132.
36. N. A. Protasenko, A. I. Poddel'sky, A. S. Bogomyakov, G. K. Fukin, V. K. Cherkasov, *Inorg. Chem.*, 2015, **54**, 6078.
37. S. E. Tolstikov, N. A. Artiukhova, G. V. Romanenko, A. S. Bogomyakov, E. M. Zueva, I. Yu. Barskaya, M. V. Fedin, K. Yu. Maryunina, E. V. Tretyakov, R. Z. Sagdeev, V. I. Ovcharenko, *Polyhedron*, 2015, **100**, 132.
38. M. Bubnov, A. Cherkasova, I. Teplova, E. Kopylova, G. Fukin, M. Samsonov, A. Bogomyakov, S. Fokin, G. Romanenko, V. Cherkasov, V. Ovcharenko, *Polyhedron*, 2016, **119**, 317.
39. M. P. Bubnov, I. A. Teplova, E. A. Kopylova, K. A. Kozhanov, A. S. Bogomyakov, M. V. Petrova, V. A. Morozov, V. I. Ovcharenko, V. K. Cherkasov, *Inorg. Chem.*, 2017, **56**, 2426.
40. N. A. Artiukhova, G. V. Romanenko, G. A. Letyagin, A. S. Bogomyakov, S. E. Tolstikov, V. I. Ovcharenko, *Russ. Chem. Bull.*, 2019, **68**, 732.
41. S. V. Tumanov, S. L. Veber, S. E. Tolstikov, N. A. Artiukhova, V. I. Ovcharenko, M. V. Fedin, *Dalton Trans.*, 2020, **49**, 5851.
42. A. A. Starikova, E. A. Metelitsa, A. G. Starikov, *J. Struct. Chem. (Engl. Transl.)*, 2019, **60**, 1219.
43. A. G. Starikov, M. G. Chegrev, A. A. Starikova, V. I. Minkin, *Russ. J. Coord. Chem.*, 2019, **45**, 675.
44. W. O. Koch, H.-J. Krüger, *Angew. Chem., Int. Ed.*, 1995, **43**, 2671.
45. W. O. Koch, V. Schünemann, M. Gerdan, A. X. Trautwein, H.-J. Krüger, *Chem. — Eur. J.*, 1998, **4**, 1255.
46. M. Graf, G. Wolmershäuser, H. Kelm, S. Demeschko, F. Meyer, H.-J. Krüger, *Angew. Chem., Int. Ed.*, 2010, **49**, 950.
47. A. G. Starikov, A. A. Starikova, V. I. Minkin, *Dokl. Chem. (Engl. Transl.)*, 2016, **467**, 83.
48. A. A. Starikova, M. G. Chegrev, A. G. Starikov, V. I. Minkin, *Comp. Theor. Chem.*, 2018, **1124**, 15.
49. T. Tezgerevska, E. Rousset, R. W. Gable, G. N. L. Jameson, E. Carolina Sañudo, A. Starikova, C. Boskovic, *Dalton Trans.*, 2019, **48**, 11674.
50. A. A. Starikova, M. G. Chegrev, A. G. Starikov, *Russ. Chem. Bull.*, 2020, **69**, 203.
51. A. A. Starikova, M. G. Chegrev, A. G. Starikov, *Russ. J. Coord. Chem.*, 2020, **46**, 193.
52. V. I. Minkin, A. A. Starikova, M. G. Chegrev, A. G. Starikov, *Russ. J. Coord. Chem.*, 2020, **46**, 371.
53. T. Bally, *Nat. Chem.*, 2010, **2**, 165.
54. M. J. Frisch, G. W. Trucks, H. B. Schlegel, G. E. Scuseria, M. A. Robb, J. R. Cheeseman, G. Scalmani, V. Barone, G. A. Petersson, H. Nakatsuji, X. Li, M. Caricato, A. V. Marenich, J. Bloino, B. G. Janesko, R. Gomperts, B. Mennucci, H. P. Hratchian, J. V. Ortiz, A. F. Izmaylov, J. L. Sonnenberg, D. Williams-Young, F. Ding, F. Lipparini, F. Egidi, J. Goings, B. Peng, A. Petrone, T. Henderson, D. Ranasinghe, V. G. Zakrzewski, J. Gao, N. Rega, G. Zheng, W. Liang, M. Hada, M. Ehara, K. Toyota, R. Fukuda, J. Hasegawa, M. Ishida, T. Nakajima, Y. Honda, O. Kitao, H. Nakai, T. Vreven, K. Throssell, J. A. Montgomery, Jr., J. E. Peralta, F. Ogliaro, M. J. Bearpark, J. J. Heyd, E. N. Brothers, K. N. Kudin, V. N. Staroverov, T. A. Keith, R. Kobayashi, J. Normand, K. Raghavachari, A. P. Rendell, J. C. Burant, S. S. Iyengar, J. Tomasi, M. Cossi, J. M. Millam, M. Klene, C. Adamo, R. Cammi, J. W. Ochterski, R. L. Martin, K. Morokuma, O. Farkas, J. B. Foresman, D. J. Fox, *Gaussian 16 (Revision A.03)*, Gaussian, Inc., Wallingford (CT), 2016.
55. J. M. Tao, J. P. Perdew, V. N. Staroverov, G. E. Scuseria, *Phys. Rev. Lett.*, 2003, **91**, 146401.
56. V. N. Staroverov, G. E. Scuseria, J. Tao, J. P. Perdew, *J. Chem. Phys.*, 2003, **119**, 12129.
57. G. K. Gransbury, B. N. Livesay, J. T. Janetzki, M. A. Hay, R. W. Gable, M. P. Shores, A. Starikova, C. Boskovic, *J. Am. Chem. Soc.*, 2020, **142**, 10692.
58. V. I. Minkin, A. G. Starikov, A. A. Starikova, *Pure Appl. Chem.*, 2018, **90**, 811.
59. L. Noodleman, *J. Chem. Phys.*, 1981, **74**, 5737.
60. M. Shoji, K. Koizumi, Y. Kitagawa, T. Kawakami, S. Yamamoto, M. Okumura, K. Yamaguchi, *Chem. Phys. Lett.*, 2006, **432**, 343.
61. *Chemcraft, version 1.7*, 2013; <http://www.chemcraftprog.com>.
62. M. P. Bubnov, N. A. Skorodumova, A. S. Bogomyakov, G. V. Romanenko, A. V. Arapova, K. A. Kozhanov, N. N. Smirnova, G. A. Abakumov, V. K. Cherkasov, *Russ. Chem. Bull.*, 2011, **60**, 449.
63. E. Yu. Fursova, O. V. Kuznetsova, E. V. Tretyakov, G. V. Romanenko, A. S. Bogomyakov, V. I. Ovcharenko, R. Z. Sagdeev, V. K. Cherkasov, M. P. Bubnov, G. A. Abakumov, *Russ. Chem. Bull.*, 2011, **60**, 809.
64. S. V. Fokin, E. Yu. Fursova, G. A. Letyagin, A. S. Bogomyakov, V. A. Morozov, G. V. Romanenko, V. I. Ovcharenko, *J. Struct. Chem. (Engl. Transl.)*, 2020, **61**, 541.
65. V. I. Minkin, A. G. Starikov, A. A. Starikova, O. A. Gapurenko, R. M. Minyaev, A. I. Boldyrev, *Phys. Chem. Chem. Phys.*, 2020, **22**, 1288.

66. A. A. Starikova, A. G. Starikov, V. I. Minkin, *Russ. Chem. Bull.*, 2016, **65**, 1464.
67. T. Glaser, H. Theil, I. Liratzis, T. Weyhermüller, E. Bill, *Inorg. Chem.*, 2006, **45**, 4889.
68. E. V. Tretyakov, V. I. Ovcharenko, *Russ. Chem. Rev.*, 2009, **78**, 971.
69. *Stable Radicals: Fundamental and Applied Aspects of Odd-electron Compounds*, Ed. R. Hicks, Wiley, Chichester, 2011, 588 pp.
70. E. V. Tret'yakov, V. G. Vasil'ev, A. S. Bogomyakov, G. V. Romanenko, M. V. Fedin, I. S. Antipin, S. E. Solov'eva, A. I. Konovalov, R. Z. Sagdeev, V. I. Ovcharenko, *Russ. Chem. Bull.*, 2013, **62**, 543.

*Received November 18, 2020;  
in revised form December 18, 2020;  
accepted December 23, 2020*